Available online at www.sciencedirect.com
SCIENCE DIRECT®
Physics Letters A 343 (2005) 417–422
PHYSICS LETTERS A
www.elsevier.com/locate/pla

Bifurcations from stationary to pulsating solitons in the cubic–quintic complex Ginzburg–Landau equation

Eduard N. Tsoy [*,1], Nail Akhmediev

Optical Sciences Group, Research School of Physical Sciences and Engineering, The Australian National University, Canberra, ACT 0200, Australia

Received 4 May 2005; accepted 10 May 2005
Available online 1 July 2005
Communicated by V.M. Agranovich

Abstract

Stationary to pulsating soliton bifurcation analysis of the complex Ginzburg–Landau equation (CGLE) is presented. The analysis is based on a reduction from an infinite-dimensional dynamical dissipative system to a finite-dimensional model. Stationary solitons, with constant amplitude and width, are associated with fixed points in the model. For the first time, *pulsating* solitons are shown to be stable *limit cycles* in the finite-dimensional dynamical system. The boundaries between the two types of solutions are obtained approximately from the reduced model. These boundaries are reasonably close to those predicted by direct numerical simulations of the CGLE.

PACS: 04.30.Nk; 05.45.Yv; 42.65.Sf; 42.65.Tg

The complex Ginzburg–Landau equation (CGLE) is one of the basic equations for modelling modulated amplitude waves [1], spatio-temporal dynamics and spontaneous development of coherent structures in a variety of nonlinear dissipative systems [2,3]. Examples include pulse generation by passively mode-locked soliton lasers [4], signal transmission in all-optical communication lines [5], travelling waves in binary fluid mixtures [6], and also pattern formation in many other physical systems [7]. Complicated patterns consist of simpler localized solutions like fronts, pulses, sources and sinks [8].

Pulsating soliton solutions of dissipative systems have attracted a great deal of attention in recent years. They have been found numerically [9–11] and observed experimentally [11] in a fiber laser. Pulsating solitons form one set of possible localized solutions of the CGLE, and they exist on an equal basis with stationary solitons. Such localized waves exist, in various forms in biology, chemistry and physics.

* Corresponding author.
E-mail address: etsoy@physic.uzsci.net (E.N. Tsoy).
1 Also at: Physical-Technical Institute of the Uzbek Academy of Sciences, Tashkent, Uzbekistan.

0375-9601/$ – see front matter
doi:10.1016/j.physleta.2005.05.102

A pulsating soliton can be described as a limit cycle of an infinite-dimensional dissipative dynamical system [12]. It is different from the higher-order solitons that are usually connected with an integrable model [13]. Although numerical simulations show clearly the existence of pulsating solutions and their bifurcations from stationary solitons, so far there has been no progress in finding analytic expressions for pulsating solutions and bifurcation boundaries. The problem is not simple as there are several parameters of the CGLE that define the regions of existence for both stationary and pulsating solitons. Hence, the bifurcation boundaries are surfaces in this multi-dimensional space of the parameters.

In this work we use a reduction from an infinite-dimensional to a five-dimensional model, and we aim to find localized solutions of the CGLE and the transformations that they are subjected to when the system parameters are varied. Although exact solutions of the CGLE do exist [3], they can be presented explicitly only for certain relations between the parameters of the equation. Furthermore, only stationary solutions can be found. Hence, we are faced with the necessity of finding an efficient approximation to tackle the problem. We have found that the method of moments, originally developed by Maimistov [14] for the perturbed nonlinear Schrödinger equation (NLSE) can be used for solving our problem. The moments are the integral characteristics of the field under consideration. In principle, there are an infinite number of equations for moments. One can obtain exact results by using the complete set of these equations. However, in practice, one uses a trial function with a finite number of parameters, and this is the way to obtain a significant reduction in the number of variables used for the description of the dynamics.

The cubic–quintic complex Ginzburg–Landau equation, in dimensionless form, is written as

$$\begin{aligned} i\psi_t + \frac{D}{2}\psi_{xx} + |\psi|^2\psi &= -\nu|\psi|^4\psi + i\delta\psi + i\epsilon|\psi|^2\psi \\ &\quad + i\beta\psi_{xx} + i\mu|\psi|^4\psi \\ &\equiv R[\psi], \end{aligned} \tag{1}$$

where $\psi(x,t)$ is the normalized envelope of the field, t and x are time and spatial variables, respectively, D is the group velocity dispersion coefficient, ν is the parameter of the quintic nonlinearity, δ represents the linear loss, ϵ is the nonlinear gain coefficient, β stands for the spectral filtering, and μ characterizes the saturation of the nonlinear gain. Stable soliton solutions of the CGLE exist only for the following choices for the signs of the coefficients: $\delta, \mu < 0$, $\beta, \epsilon > 0$, and any sign for ν and D (see, e.g., [3,10]). Hence, in this work, we limit ourselves only to this range.

The method of moments [14] is a reduction of the complete problem of the evolution of a field that has an infinite number of degrees of freedom to the evolution of a finite set of pulse characteristics. For a localized solution with a single maximum, these include the peak amplitude, pulse width and center-of-mass position. For an arbitrary localized field, the two integrals, namely the energy Q and momentum P

$$Q = \int_{-\infty}^{\infty} |\psi|^2\,dx,$$

$$P = \frac{1}{2}\int_{-\infty}^{\infty} \left(\psi\psi_x^* - \psi^*\psi_x\right)dx \tag{2}$$

are two basic variables evolving with t. Three higher-order generalized moments, related to the pulse, are given by the following expressions [14]:

$$I_1 = \int_{-\infty}^{\infty} x|\psi|^2\,dx, \qquad I_2 = \int_{-\infty}^{\infty} (x-x_0)^2|\psi|^2\,dx,$$

$$I_3 = \int_{-\infty}^{\infty} (x-x_0)\left(\psi^*\psi_x - \psi\psi_x^*\right)dx, \tag{3}$$

where $x_0(t) = I_1/Q$. Using Eq. (1) one can derive the evolution equations for the generalized moments. For the five integrals given above, one can obtain the following [14]:

$$\frac{dQ}{dt} = i\int_{-\infty}^{\infty} \left(\psi R^* - \psi^* R\right)dx,$$

$$\frac{dP}{dt} = -i\int_{-\infty}^{\infty} \left(\psi_x R^* + \psi_x^* R\right)dx,$$

$$\frac{dI_1}{dt} = iDP + i\int_{-\infty}^{\infty} x\left(\psi R^* - \psi^* R\right)dx,$$

$$\frac{dI_2}{dt} = -iDI_3 + i\int_{-\infty}^{\infty}(x-x_0)^2\big(\psi R^* - \psi^* R\big)\,dx,$$

$$\frac{dI_3}{dt} = 2P\frac{dx_0}{dt} + i\int_{-\infty}^{\infty}\big(2D|\psi_x|^2 - |\psi|^4\big)\,dx + 2i\int_{-\infty}^{\infty}(x-x_0)\big(\psi_x R^* + \psi_x^* R\big)\,dx + i\int_{-\infty}^{\infty}\big(\psi R^* + \psi^* R\big)\,dx. \quad (4)$$

Eqs. (4) are general in the sense that they are valid for a large class of NLSE-type evolution equations, including Eq. (1) with arbitrary coefficients as a particular case. If we use an exact solution of Eq. (1), ψ, then Eqs. (4) are exact.

For problems of a certain class, even the first two equations (4) may be sufficient when one deals with exact two-parameter reductions of the CGLE solutions [15]. In Ref. [15], such an approach was used to find the CGLE solutions in the form of stable soliton pairs and trains. The method of moments has also been applied to find stationary solutions of the CGLE (1) in Ref. [16] although there was no attempt at finding pulsating solitons. Our tests showed that five is the minimum number of moments needed to describe pulsating solitons using the reduced system. Having more of them may improve the accuracy, but the complexity of the analysis then increases dramatically.

The choice of the trial function is crucial for obtaining solutions with the desired properties. Any reduction from an infinite-dimensional to a finite-dimensional system will have deficiencies. In approaches like this, the choice of the trial function can only be justified at the last stage of analysis, when the approximate solutions are compared with numerical simulations of the original equation. We use the fact that soliton solutions remain localized even when they are pulsating. Therefore, we take the sech-function:

$$\psi(x,t) = A\,\mathrm{sech}\left(\frac{x-x_0}{w}\right) \times \exp\big\{i\big[b(x-x_0) + c(x-x_0)^2\big]\big\}, \quad (5)$$

where $A(t)$, $w(t)$ and $x_0(t)$ are the amplitude, width and maximum position of the pulse, respectively, $b(t)$ is the soliton velocity and $c(t)$ is the chirp parameter. The chirp is highly important, as the numerical simulations [10,11] show. The number of parameters in the trial function must correspond to the number of moments used in the set of equations (4). More complicated trial functions need more equations in (4).

Now, the generalized moments can be expressed in terms of the variable parameters of the trial function. Evaluation of the integrals (2) and (3), with a help of Eq. (5), gives the following expressions:

$$Q = 2A^2 w, \qquad P = -2iA^2 wb, \qquad I_1 = 2A^2 w x_0,$$
$$I_2 = \frac{\pi^2}{6}A^2 w^3, \qquad I_3 = i\frac{2\pi^2}{3}A^2 w^3 c. \quad (6)$$

Then, using Eqs. (4), one can obtain a set of ordinary differential equations for the soliton parameters Q, w, c, x_0 and b:

$$Q_t = F_1 \equiv 2Q\left[\delta - \beta b^2 + \frac{\epsilon}{3}\frac{Q}{w} + \frac{2\mu Q^2 - 5\beta}{15w^2} - \frac{\pi^2}{3}\beta c^2 w^2\right],$$

$$w_t = F_2 \equiv -\frac{2\epsilon}{\pi^2}Q + \frac{8\beta - \mu Q^2}{\pi^2 w} + 2Dcw - \frac{16\pi^2}{15}\beta c^2 w^3,$$

$$c_t = F_3 \equiv -2Dc^2 - \frac{1}{\pi^2 w^2}\left[4\left(\frac{\pi^2}{3}+1\right)\beta c + \frac{Q}{w} + \frac{8\nu Q^2 - 30D}{15w^2}\right],$$

$$x_{0,t} = F_4 \equiv b\left(D - \frac{2\pi^2}{3}\beta c w^2\right),$$

$$b_t = F_5 \equiv -\frac{4}{3}\beta\left(\frac{1}{w^2} + \pi^2 c^2 w^2\right)b. \quad (7)$$

Fixed points (FPs) of the dynamical system (7) can be found from the set of algebraic equations $F_j = 0$, $j = 1,\dots,5$. The stability of the FPs is determined from the analysis of eigenvalues λ_j, $j = 1, \dots, 5$, of the Jacobian matrix $M_{ij} = \partial F_i/\partial p_j$, where $\{p_1,\dots,p_5\} \equiv \{Q, w, c, x_0, b\}$, and $i = 1,\dots,5$. If the real part of at least one eigenvalue is positive, then the corresponding fixed point is unstable. In principle, the whole five-dimensional dynamical system (7) can be studied using the specialized software [17]. We analyse the system based on general theory and using further simplifications.

Firstly, we consider solutions with $b = 0$ in Eqs. (7). The real part of the eigenvalue which corresponds to b is negative for any set of the system parameters. The soliton center, $x_0(t)$, takes a constant value for $t \to \infty$ and the real part of the corresponding eigenvalue is zero (neutral stability). Therefore, we can make a further reduction and consider a system with only three variables, viz. Q, w, and c. We denote the three corresponding eigenvalues by λ_1, λ_2 and λ_3. Note that, since the characteristic equation for these eigenvalues is cubic, then either $\lambda_1 = \lambda_2^*$ and λ_3 is real, or all three λ_i are real.

We find FPs numerically by solving the algebraic equations, and calculate the characteristic eigenvalues by analyzing the Jacobian matrix. In this way, we have identified the regions where solutions have distinctive features. The bifurcation diagram for the dynamical system (7) in the (ν, ϵ)-plane is presented in Fig. 1. We take $D = 1$ and $\delta = -0.1$ henceforth in the Letter. To facilitate comparison with exact results, the parameters of the model are chosen to be the same as in the numerical simulations of Ref. [10], namely, $\mu = -0.1$ and $\beta = 0.08$.

When the value of the gain ϵ is small, there are no stable or unstable FPs (i.e., no stationary solitons) in the system. This region is located below $\epsilon = 0.6$, and therefore it is not shown in Fig. 1. For moderate values of ϵ, there are two FPs. In the region below the curve 1 in Fig. 1(a), one FP is stable while the other one is unstable. The signs of the real and imaginary parts of the eigenvalues, for the stable FP in this region are the following:

$$\mathrm{Re}[\lambda_{1,2}] < 0, \qquad \mathrm{Im}[\lambda_1] = -\mathrm{Im}[\lambda_2],$$
$$\mathrm{Re}[\lambda_3] < 0, \qquad \mathrm{Im}[\lambda_3] = 0.$$

The stable FP corresponds to a stationary CGLE soliton with constant soliton parameters p_j.

Curve 1 in Fig. 1(a) is the bifurcation boundary (threshold) where the stable fixed point turns into an unstable one. Above curve 1,

$$\mathrm{Re}[\lambda_{1,2}] > 0, \qquad \mathrm{Im}[\lambda_1] = -\mathrm{Im}[\lambda_2],$$
$$\mathrm{Re}[\lambda_3] < 0, \qquad \mathrm{Im}[\lambda_3] = 0.$$

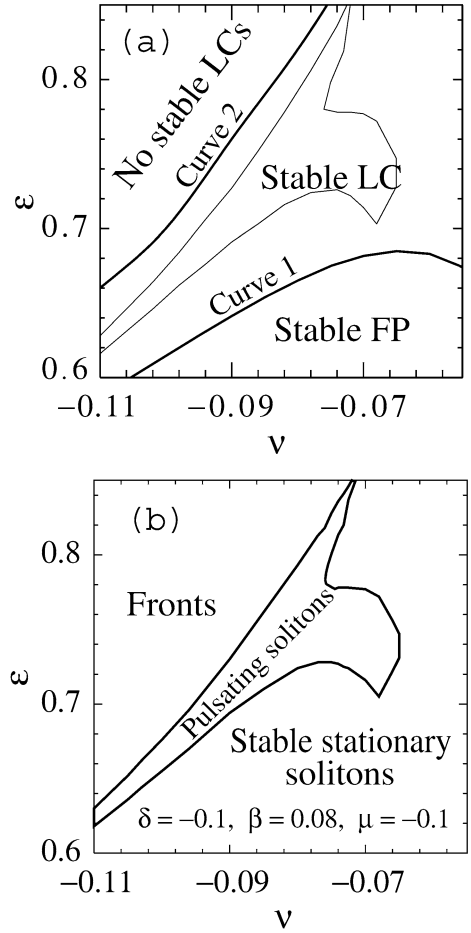

Fig. 1. (a) Regions of existence and stability of FPs and limit cycles (LCs) of the reduced system in (ν, ϵ)-plane. The central region, between the two solid lines 1 and 2, corresponds to stable LC. (b) Regions of existence for various soliton solutions obtained from numerical simulations of CGLE (1). The region for pulsating solitons, found numerically in Ref. [10], is copied from (b) to (a) for comparison. The parameters of the dynamical system are shown in (b).

On line 1, a stable FP is transformed into a stable limit cycle (LC) and an unstable FP. We confirmed, numerically, that the *stable* limit cycle of model (7) does indeed exist between the solid curves 1 and 2. Two examples of LC in (Q, w, c)-space are shown in Fig. 2(a) and (b). The limit cycle has zero size on line 1 in Fig. 1(a). This corresponds to a super-critical Hopf bifurcation [18]. The limit cycle elongates in Q axis direction when ϵ increases. It becomes infinitely large and breaks off on line 2 in Fig. 1(a).

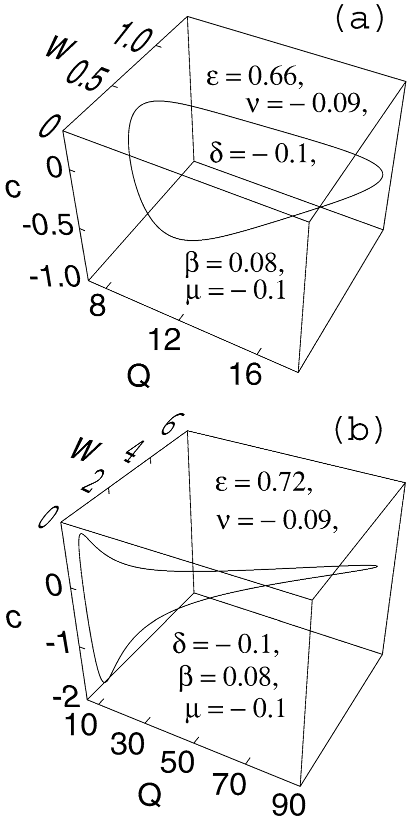

Fig. 2. Two examples of stable limit cycle of the system (7) in (Q, w, c)-space. The parameters are shown in (a) and (b), respectively. Note the different scales for the axes in (a) and (b).

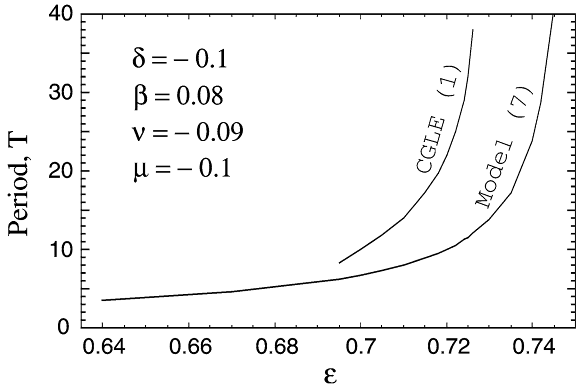

Fig. 3. Period of pulsations T versus ϵ. Upper curve correspond to exact numerical results while the lower curve describes the data obtained from the low-dimensional model.

The smaller region in Fig. 1(a) surrounded by the light solid curve, is copied from Fig. 1(b) for comparison. This is the boundary for the existence of pulsating solitons found by direct numerical simulations of CGLE (1). One can see that the thresholds (solid curves 1 and 2) of the existence of the stable LC provide reasonably good estimates for the boundaries.

The period of oscillations, T, depends on the parameters of the system. A plot of T versus ϵ at constant $\nu = -0.09$ is given in Fig. 3. The upper curve represents the results of exact numerical simulations of the CGLE, while the lower curve shows the period of oscillations found from our finite-dimensional model. There is an apparent difference in the values found for the period, due to the drastic reduction in the number of degrees of freedom in the model. However, the two curves have the same qualitative behaviour. In particular, each curve starts with a finite value of the period T at the lower boundary of the region where pulsating solitons exist, and increases to infinity at the upper boundary.

Above the curve 2, the soliton amplitude $A = [Q/(2w)]^{1/2}$ remains almost constant, but the soliton energy Q and the width w increase monotonically with t. This motion is tantamount to the localized solution of CGLE with constant amplitude and the width that increases indefinitely. The final stage of this motion is an asymptotic transformation of the soliton into two separating fronts with constant velocities. Thus, the qualitative agreement above the line 2 is also fairly good and the main features of the dynamics are captured correctly.

Another slice of the parameter space, namely the (μ, ϵ)-plane, is shown in Fig. 4(a). As in Fig. 1(a), there are two FPs in the region presented. One of them is always unstable. The stable FP exists below the solid curve 1. The bifurcation on the curve 1 is the same as that in Fig. 1(a). The solid curve 2 corresponds to the transition between limit cycles and the solutions with increasing width. From Fig. 1 and Fig. 4, one can see that the results obtained from the model (7) for pulsating solitons and the boundaries for their existence are in reasonable agreement with direct numerical simulations of the CGLE over a wide range of the system parameters.

Thus, considering the evolution of the dissipative soliton profile, the model (7) is able to predict:

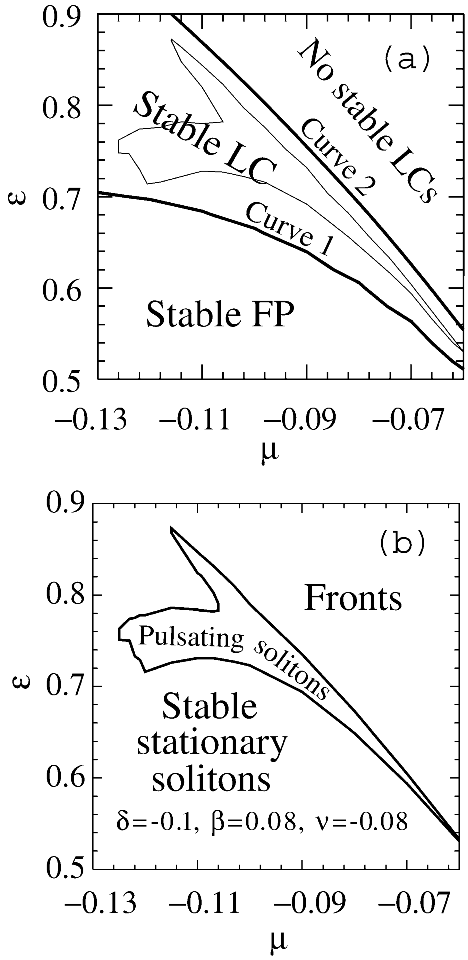

Fig. 4. (a) Diagram of existence and stability of FPs and LCs of the reduced model in the (μ, ϵ)-plane. Stable LCs exist between the curves 1 and 2. (b) Existence diagram based on numerical simulations of CGLE [10]. The solid curve bounding the region for pulsating solitons in (b) is copied to (a) for comparison. The parameters of the dynamical system are shown in (b).

(a) stable and unstable stationary solitons;
(b) periodic soliton pulsations;
(c) the unlimited increase in the soliton width at constant amplitude (which is equivalent to splitting solitons into moving fronts);
(d) bifurcations between these dynamical behaviours.

In summary, we have derived a finite-dimensional dynamical system associated with the CGLE. We have demonstrated that the pulsating solitons of the CGLE correspond to the limit cycles of this system, while stationary solitons of the CGLE are related to the fixed points. We have found the approximate bifurcation boundaries between different types of solutions in the parameter space.

Acknowledgements

This work was funded by the Australian Research Council. The authors are grateful to Dr. A. Ankiewicz for a critical reading of the manuscript.

References

[1] L. Brusch, A. Torcini, M. van Hecke, M.G. Zimmermannf, M. Bär, Physica D 160 (2001) 127.
[2] I.S. Aranson, L. Kramer, Rev. Mod. Phys. 74 (2002) 100.
[3] See, e.g., N. Akhmediev, A. Ankiewicz, Solitons: Nonlinear Pulses and Beams, Chapman & Hall, London, 1997;
G.P. Agrawal, Nonlinear Fiber Optics, Academic Press, London, 1989.
[4] E.P. Ippen, Appl. Phys. B 58 (1994) 159.
[5] Z. Bakonyi, D. Michaelis, U. Peschel, G. Onishchukov, F. Lederer, J. Opt. Soc. Am. B 19 (2002) 487.
[6] P. Kolodner, Phys. Rev. Lett. 66 (1991) 1165.
[7] M.C. Gross, P.C. Hohenberg, Rev. Mod. Phys. 65 (1993) 851.
[8] W. van Saarlos, P.C. Hohenberg, Physica D 56 (1992) 303.
[9] R.J. Deissler, H.R. Brand, Phys. Rev. Lett. 72 (1994) 478.
[10] N. Akhmediev, J.M. Soto-Crespo, G. Town, Phys. Rev. E 63 (2001) 056602.
[11] J.M. Soto-Crespo, M. Grapinet, Ph. Grelu, N. Akhmediev, Phys. Rev. E 70 (2004) 066612.
[12] N. Akhmediev, A. Ankiewicz, Dissipative solitons in the complex Ginzburg–Landau and Swift–Hohenberg equations, in: Dissipative Solitons, Springer, Heidelberg, 2005.
[13] J. Satsuma, N. Yajima, Prog. Theor. Phys. Suppl. 55 (1974) 284.
[14] A.I. Maimistov, J. Exp. Theor. Phys. 77 (1993) 727, Zh. Eksp. Teor. Fiz. 104 (1993) 3620 (in Russian).
[15] N. Akhmediev, A. Ankiewicz, J.M. Soto-Crespo, J. Opt. Soc. Am. B 15 (1998) 515.
[16] M.N. Zhuravlev, N.V. Ostrovskaya, J. Exp. Theor. Phys. 99 (2004) 427, Zh. Eksp. Teor. Fiz. 126 (2004) 483 (in Russian).
[17] See, e.g., the software "AUTO2000" on the web page http://indy.cs.concordia.ca/auto/.
[18] J. Guckenheimer, P. Holmes, Nonlinear Oscillations, Dynamical Systems and Bifurcations of Vector Fields, Springer-Verlag, New York, 1983.